Quantum fast Fourier transform using multilevel atoms

Ashok Muthukrishnan* and C. R. Stroud, Jr.
The Institute of Optics, University of Rochester, Rochester, New York 14627
(August 27, 2001)

We propose an implementation of the quantum fast Fourier transform algorithm in an entangled system of multilevel atoms. The Fourier transform occurs naturally in the unitary time evolution of energy eigenstates and is used to define an alternate wave-packet basis for quantum information in the atom. A change of basis from energy levels to wave packets amounts to a discrete quantum Fourier transform within each atom. The algorithm then reduces to a series of conditional phase transforms between two entangled atoms in mixed energy and wave-packet bases. We show how to implement such transforms using wave-packet control of the internal states of the ions in the linear ion-trap scheme for quantum computing.

arXiv:quant-ph/0112017v1 3 Dec 2001

1. INTRODUCTION

The discrete quantum Fourier transform,

$$\mathrm{DFT}_N : \ |a\rangle \mapsto \frac{1}{\sqrt{N}} \sum_{c=0}^{N-1} \exp(i2\pi ac/N)\,|c\rangle, \qquad (1)$$

which links two sets of states each labeled by integers, occurs in many applications of quantum computing [1]. It is central to Shor's algorithm for prime factorization [2], which has applications in public-key cryptography [3]. Coppersmith [4] describes an efficient algorithm for implementing this transform when N is a power of 2, achieving an exponential speed-up over the classical fast Fourier transform (FFT) algorithm [5].

Advances in quantum FFT technology have been motivated by the difficulty of implementing quantum logic between macroscopically distinct two-level systems, or qubits. The difficulty arises from decoherence, the loss of coherence in a quantum superposition due to coupling with the environment. It is known that one-qubit gates alone, interspersed by classical measurements, suffice to build the quantum FFT [6], but this result is hard to implement in practice. Approximate simulations of DFT_N have also been proposed [4,7], and are known to be more tolerant to phase fluctuations in the two-qubit gates when applied in the context of Shor's algorithm [8].

In this paper, we consider an analogue of the exact quantum FFT algorithm based on multi-valued quantum logic [9], and propose a novel realization of DFT_N in multilevel atomic systems using wave-packet control methods. The advantage of using $d > 2$ computational levels in each atom is that the number of atoms needed for the algorithm is reduced by a factor of $\log_2 d$. For example, $d = 8$ levels stores three qubits of information in each atom, requiring only $Q/3$ atoms for computing DFT_N for $N = 2^Q$. Since fewer atoms are needed, the multilevel approach minimizes the decoherence associated with the macroscopic entanglement of these atoms, and enables a scale-up in the implementation of the quantum FFT.

In section 2, we show that the elementary operations needed for the algorithm are a Fourier transform of the d levels in each atom, DFT_d, and a phase gate that couples two atoms together. The d-level Fourier transform takes the place of the Walsh-Hadamaard transform, which plays a prominent role in binary quantum computation [10]. The phase gate involves a conditional coupling between two entangled atoms, and is more susceptible to decoherence in implementation. As the number of phase gates in the quantum FFT scales as the square of the number of atoms, the reduction in the latter in a multilevel implementation is advantageous from a coherence-time standpoint.

We propose to implement DFT_d in the atom by a change of computational basis, as described in section 3. The Fourier transform occurs naturally in quantum mechanics in relating complementary representations and we show that this can be useful for computational purposes. A dual Fourier basis for atomic energy levels consists of localised electron wave packets at *discrete times* in one Kepler orbit about the nucleus [11]. Individual elements in the wave-packet basis can be addressed by short laser pulses that interact with the electron when it is near the atomic core. A change of basis from energy levels to wave packets effectively accomplishes DFT_d in the atom.

The quantum FFT then reduces to a sequence of controlled phase gates between two atoms in *hybrid* bases, evolving the phases of wave-packet states in one atom conditional on energy levels in the other. In section 4, we consider a method for implementing such a gate in the linear ion-trap quantum logic scheme proposed by Cirac and Zoller [12]. A multilevel phase-gate protocol in this scheme involves a sequence of laser pulses applied to two ions in the trap.

2. MULTI-VALUED QUANTUM FFT

In a system of $Q = \log_2 N$ qubits, DFT_N can be constructed using only two kinds of binary gates [4,13]. These are the single-qubit Walsh-Hadamaard transform

$$A_m = \frac{1}{\sqrt{2}} \begin{bmatrix} 1 & 1 \\ 1 & -1 \end{bmatrix}, \tag{2}$$

acting on qubit m, and the two-qubit controlled phase gate

$$B_{lm} = \begin{bmatrix} 1 & 0 & 0 & 0 \\ 0 & 1 & 0 & 0 \\ 0 & 0 & 1 & 0 \\ 0 & 0 & 0 & e^{i\phi} \end{bmatrix}, \tag{3}$$

acting on qubits l and m, where $\phi = \pi/2^{m-l}$. Specifically, it can be shown that except for a reversal of bits in the final output,

$$\begin{aligned} \mathrm{DFT}_N = (A_{Q-1}B_{Q-2,Q-1})(A_{Q-2}B_{Q-3,Q-1}B_{Q-3,Q-2}) \\ \ldots (A_1 B_{0,Q-1} B_{0,Q-2} \ldots B_{0,1}) A_0, \end{aligned} \tag{4}$$

where the sequence of gates on the right side is applied from left to right. The total number of gates is $Q(Q+1)/2 = \mathcal{O}[Q^2]$, so this is an efficient process.

To describe the multi-valued quantum FFT, we generalize the gates A_m and B_{lm} to multilevel systems. Each d-level system is referred to as a *qudit*. The states $|a\rangle$ and $|c\rangle$ in Eq. (1) can be written as a tensor product of $q = \log_d N$ qudits,

$$\begin{aligned} |a\rangle &= |a_{q-1}, a_{q-2}, \ldots, a_0\rangle, \\ a_m &= 0, 1, \ldots, d-1 \text{ for all } m, \end{aligned} \tag{5}$$

and similarly for $|c\rangle$. The numbers a_m represent the digits of a in base d. The number of qudits q in the tensor product is less than the number of qubits Q by a factor of $\log_2 d$,

$$q = \log_d N = \frac{\log_2 N}{\log_2 d} = \frac{Q}{\log_2 d}, \tag{6}$$

which reduces the number of atoms needed for the algorithm. The multi-valued analogue of the Walsh-Hadamaard transform A_m is a d-level Fourier transform,

$$\mathcal{A}_m = \mathrm{DFT}_d : \ |a_m\rangle \mapsto \frac{1}{\sqrt{d}} \sum_{b_m=0}^{d-1} \exp(i2\pi a_m b_m/d) \ |b_m\rangle, \tag{7}$$

which mixes the d states in the mth qudit, $|0\rangle, |1\rangle, \ldots, |d-1\rangle$, with phases determined by the Fourier kernel. The phase gate B_{lm} generalizes to the two-qudit gate

$$\mathcal{B}_{lm} : \ |a_l, b_m\rangle \mapsto \exp(i2\pi a_l b_m/d^{m-l+1}) \ |a_l, b_m\rangle, \tag{8}$$

which is a diagonal transformation that advances the phase of each of the d^2 states in the two-qudit basis, $|0,0\rangle, |0,1\rangle, \ldots, |d-1, d-1\rangle$, by an amount determined by the values of both qudits, a_l and b_m. For $d = 2$ and $a_l, b_m = 0$ or 1 in Eqs. (7) and (8), we recover the binary gates in Eqs. (2) and (3) respectively.

Given the above definitions for $\mathcal{A}_m$ and $\mathcal{B}_{lm}$, we show that a sequence of gates similar to that in Eq. (4) simulates DFT_N on an q-qudit register. In the multi-valued case, for $N = d^q$,

$$\begin{aligned} \mathrm{DFT}_N = (\mathcal{A}_{q-1}\mathcal{B}_{q-2,q-1})(\mathcal{A}_{q-2}\mathcal{B}_{q-3,q-1}\mathcal{B}_{q-3,q-2}) \\ \ldots (\mathcal{A}_1 \mathcal{B}_{0,q-1} \mathcal{B}_{0,q-2} \ldots \mathcal{B}_{0,1}) \mathcal{A}_0. \end{aligned} \tag{9}$$

Based on an argument given by Shor [2] for the binary quantum FFT, we consider the matrix element of DFT_N between two arbitrary states $|a\rangle$ and $|c\rangle$,

$$\langle c|\mathrm{DFT}_N|a\rangle = \frac{1}{\sqrt{N}} \exp(i2\pi ac/N), \tag{10}$$

and show that the sequence of gates in Eq. (9) has the same matrix element as above, but between states $|a\rangle$ and $|b\rangle$, where $|b\rangle$ is defined as the 'dit-reversed' version of $|c\rangle$,

$$\begin{aligned} |b\rangle &= |b_{q-1}, b_{q-2}, \ldots, b_0\rangle, \\ &= |c_0, c_1, \ldots, c_{q-1}\rangle. \end{aligned} \tag{11}$$

The least significant place in b becomes the most significant place in c, and vice versa. A reversal of qudits can be performed efficiently using multi-valued permutation gates [9], or else we can simply read out the final state in the reverse order.

To determine the amplitude $Ae^{i\phi}$ of going from $|a_{q-1}, a_{q-2}, \ldots, a_0\rangle$ to $|b_{q-1}, b_{q-2}, \ldots, b_0\rangle$ under the sequence of gates in Eq. (9), consider each set of gates separated parenthetically in this sequence. First $\mathcal{A}_m$ transforms $|a_m\rangle$ to $|b_m\rangle$ in the mth qudit with amplitude $(1/\sqrt{d}) \exp(i2\pi a_m b_m/d)$. This is followed by all the gates $\mathcal{B}_{lm}$ for $m > l$, each of which adds a phase $2\pi a_l b_m/d^{m-l+1}$ to $|a_l, b_m\rangle$ without mixing states. The net modulus A of the transition amplitude between $|a\rangle$ to $|b\rangle$ is thus determined by the product of the $\mathcal{A}_m$ gates,

$$A = \left(\frac{1}{\sqrt{d}}\right)^q = \frac{1}{\sqrt{d^q}} = \frac{1}{\sqrt{N}}. \tag{12}$$

The net phase ϕ can be separated into two parts, that due to the $\mathcal{A}_m$ gates and that due to the $\mathcal{B}_{lm}$ gates,

$$\phi = \sum_{m=0}^{q-1} 2\pi \frac{a_m b_m}{d} + \sum_{l=0}^{q-1} \sum_{m>l} 2\pi \frac{a_l b_m}{d^{m-l+1}}. \tag{13}$$

Since the first term amounts to setting $l = m$ in the second term, we can combine the terms by replacing $m > l$ with $m \geq l$ in the second summation. From Eq. (11),

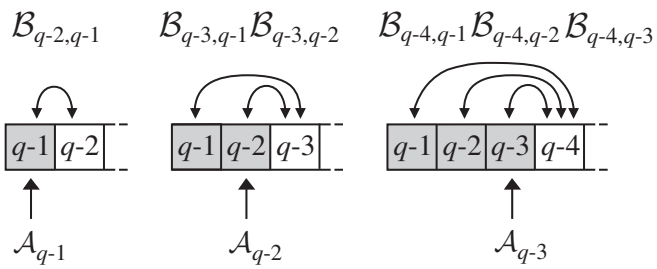

FIG. 1. Illustration of quantum FFT gates (based on Ref. [13]). The shaded squares represent the qudits transformed by $\mathcal{A}_m$, implemented as a change from the energy-level to the wave-packet basis.

we have $b_m = c_{q-1-m}$. Defining $m' = q-1-m$, the summation over $m \geq l$ becomes one over $m' < q-l$,

$$\phi = \sum_{l=0}^{q-1} \sum_{m'<q-l} 2\pi a_l c_{m'} \frac{d^{m'}}{d^{q-l}}. \tag{14}$$

Including $m' \geq q-l$ terms in the second summation above will not affect the phase since these extra terms are integer multiples of 2π. Hence, the two summations decouple to give

$$\phi = \frac{2\pi}{d^q} \sum_{l=0}^{q-1} a_l d^l \sum_{m'=0}^{q-1} c_{m'} d^{m'} = 2\pi ac/N, \tag{15}$$

where we have used $N = d^q$ and identified a and c in their base-d notation. From Eqs. (12) and (15), we see that the net amplitude of going from $|a\rangle$ to $|b\rangle$ under the sequence of gates in Eq. (9) is identical to that of going from $|a\rangle$ to $|c\rangle$ under DFT_N. Thus, to within a reversal of qudits between $|b\rangle$ and $|c\rangle$, the $q(q+1)/2$ gates in Eq. (9) simulates a quantum Fourier transform on a q-qudit register.

A graphical illustration of the quantum FFT is shown in figure 1. The first three passes through the algorithm ($m = q-1, q-2, q-3$) are shown, corresponding to the first three sets of gates in Eq. (9). During each pass, an $\mathcal{A}_m$ gate first mixes the d states in qudit m, illustrated by a shading of the respective square in the figure, followed by a sequence of $\mathcal{B}_{lm}$ gates that couple all shaded squares with the next unshaded one. In each pass, the $\mathcal{A}_m$ gate enables a d-point Fourier transform that is repeated efficiently d^m times by the conditional $\mathcal{B}_{lm}$ gates, achieving exponential speed-up over the classical FFT. The speed-up is made possible by the tensor product nature of quantum entanglement [14]. In the multi-valued case, this corresponds to a d-ary tree decomposition of DFT_N in terms of unitary operations.

At the completion of the quantum FFT, each qudit is read out by measurement. For a single multilevel system, this yields one value per qudit, corresponding to one of the d computational levels. Information stored in a superposition of these levels is lost upon measurement, analogously to the situation in a two-level system. The measured output of the multi-valued algorithm is thus always a product state of the q qudits, corresponding to a classical number in base d.

3. ATOMIC FOURIER TRANSFORM

Consider the implementation of the transform $\mathcal{A}_m$ in an atom with d computational levels. As shown in Eq. (7), this transform uniformly mixes all the levels in the atom with phases determined by the Fourier kernel. In the basis of energy levels, this requires precise control of the relative phases of the levels. Such control is not feasible for large numbers of levels in the energy basis. However, we can regard this as a problem in wave-packet control. Atomic wave packets are superpositions of energy levels with different phase relations among the levels. We propose to implement DFT_d in the atom by means of a dual computational basis composed of wave packets [11].

3.1. Energy and wave packet bases

The Fourier transform occurs naturally in the change of state representation from coordinate to momentum in quantum mechanics. Although time is not an observable, we can also speak of an uncertainty relation between energy and time. In this case, the Fourier kernel appears in the unitary time-evolution operator, which relates the continuous dynamics of the bound atomic state to its discrete energy spectrum. A larger number of energy levels in the superposition leads to a greater localization in the wave packet. By appropriately discretizing the dynamics, we can define a wave-packet basis in the atom that is related to the energy-level basis by a discrete quantum Fourier transform.

Consider radial wave packets [15], which are superpositions of Rydberg energy levels with low angular momentum. These levels have long radiative life times, approaching a millisecond for principal quantum number $n > 100$. Take d energy levels centered at $\bar{n}$ with angular momentum $l = 1$ to represent the computational basis in the atom,

$$|j\rangle_\nu = |\bar{n}+j, 1, 0\rangle, \tag{16}$$
$$j = -d/2+1, -d/2+2, \ldots, d/2,$$

where the subscript ν denotes a state in the energy-level basis. We have assumed above that $\bar{n}$ is an integer and d is an even number for simplicity, but the arguments below are easily extended to non-integer $\bar{n}$ and odd d. A uniform superposition of the d levels corresponds to a radially-localized wave packet in space whose time evolution is given by

$$|\psi(t)\rangle = \frac{1}{\sqrt{d}} \sum_j \exp(-i\omega_j t)\, |j\rangle_\nu, \tag{17}$$

where $\hbar\omega_j$ is the energy of the jth level in the superposition, and $\hbar\omega_0$ is the mean energy of the wave packet corresponding to principal quantum number $\bar{n}$. To separate the classical and revival dynamics of the wave packet, we expand $\omega_j - \omega_0$ in a Taylor series in $j = n - \bar{n}$,

$$\omega_j - \omega_0 = 2\pi \left[\frac{j}{T_K} - \frac{j^2}{2! T_{\rm rev}} + \frac{j^3}{3! T_{\rm sr}} - \cdots \right]. \tag{18}$$

The Kepler period $T_K = 2\pi\bar{n}^3$ (in atomic units) measures the round-trip time for the wave packet traveling between the inner and outer turning points of the classical orbit. This corresponds to a radial shell of probability distribution varying periodically in size. The revival time $T_{\rm rev}$ and the super-revival time $T_{\rm sr}$ describe higher-order effects such as dispersion and revivals.

Define an orthogonal basis of wave-packet states corresponding to d discrete times during the classical Kepler evolution of the radial wave packet [11],

$$\begin{aligned} |k\rangle_\tau &= \frac{1}{\sqrt{d}} \sum_j \exp(-i2\pi jk/d)\, |j\rangle_\nu \\ &\approx |\psi(kT_K/d)\rangle, \end{aligned} \tag{19}$$

where $k = -d/2+1, -d/2+2, \ldots, d/2$, and the subscript τ denotes a state in the wave-packet basis. Thus $k = 0$ corresponds to the wave-packet state centered at the inner turning point of the classical orbit, and $k = \pm|k|$ correspond to wave-packet states moving in opposite directions at some intermediate location in the orbit, as illustrated in figure 2.

The energy-level basis $|j\rangle_\nu$ is related to the wave-packet basis $|k\rangle_\tau$ by a d-level Fourier transform,

$$\begin{aligned} \mathcal{A}_m |j\rangle_\nu &= \frac{1}{\sqrt{d}} \sum_{j'} \exp(i2\pi jj'/d)\, |j'\rangle_\nu \\ &= |k = -j\rangle_\tau, \end{aligned} \tag{20}$$

where we have used Eqs. (7) and (19). This suggests that $\mathcal{A}_m$ can be implemented in the atom by a change of computational basis from that of energy eigenstates to that of wave-packet states. A change of basis does not involve any free time evolution or real-time processing in the atom, which means that there is no computational cost to realizing the $\mathcal{A}_m$ gates in this manner.

To understand the effect of the basis change on the algorithm, we refer again to figure 1. Recall that the shading of each square in the figure corresponds to the application of a $\mathcal{A}_m$ gate to that qudit in the array, and the following $\mathcal{B}_{lm}$ gates in that pass through the algorithm couple all the shaded squares with the next unshaded one. If $\mathcal{A}_m$ is regarded as a change of basis from energy levels to wave packets, then the shaded squares are to be read in the wave-packet basis. Consequently, each $\mathcal{B}_{lm}$ gate involves different bases for the two qudits l and m in the transformation. The quantum FFT thus reduces to a series of conditional two-qudit phase transforms $\mathcal{B}_{lm}$ performed in hybrid bases.

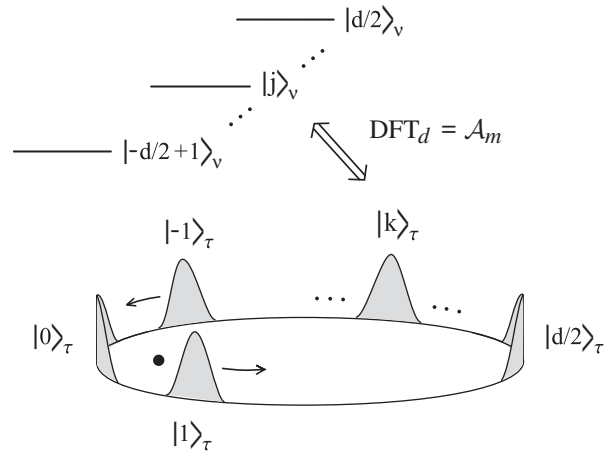

FIG. 2. The Fourier conjugate of the energy-level basis $|j\rangle_\nu$ consists of wave-packet states $|k\rangle_\tau$ evenly distributed in time around a classical orbit. A radial wave-packet basis can be thought of as an ensemble of such orbits with different orientations for the ellipses.

In the atomic case, $\mathcal{B}_{lm}$ can be regarded as phase shifts applied to each wave-packet state $|k\rangle_\tau$ in the mth atom conditional on each energy eigenstate $|j\rangle_\nu$ in the lth atom. In view of Eq. (20), we rewrite Eq. (8) as

$$\begin{aligned} \mathcal{B}_{lm}: \ |j\rangle_\nu |k\rangle_\tau &\mapsto \exp(i\phi_{jk})\, |j\rangle_\nu |k\rangle_\tau, \\ \phi_{jk} &= -2\pi jk/d^{m-l+1}. \end{aligned} \tag{21}$$

We describe a protocol for implementing $\mathcal{B}_{lm}$ in a linear ion trap in section 4. This requires coherent control of the wave-packet basis in the target atom, which we discuss below.

3.2. Coherent wave packet control

Consider an arbitrary Rydberg state in the wave-packet basis,

$$|\psi(t)\rangle = \exp(-i\omega_0 t) \sum_k \tilde{b}_k(t)\, |k\rangle_\tau, \tag{22}$$

where $\tilde{b}_k$ are slowly varying amplitudes from which we have removed the average frequency ω_0 corresponding to the mean Rydberg level $\bar{n}$ in Eq. (16). Since the wave-packet states are not stationary, the amplitudes $\tilde{b}_k$ evolve in time. During a Kepler period, the periodic motion of the radial wave packet corresponds to a cyclic permutation in the amplitudes,

$$\tilde{b}_k(mT_K/d) = \tilde{b}_{k-m}(0), \tag{23}$$

where m is an integer and $k-m$ is taken modulo d. At later times, higher-order terms in the Taylor expansion of Eq. (18) become significant, and the dispersion of the Rydberg wave function mixes the amplitudes $\tilde{b}_k$ nontrivially. However at the revival times $T_{\rm rev}$, the wave function reforms into the original state and nearly recovers the initial distribution of amplitudes in the wave-packet basis.

An applied laser field interacts strongly with a Rydberg wave packet when it is near the atomic core. This phenomenon underlies the excitation and photo-ionization of radial wave packets [16], and we use this as a means for coherent control of individual amplitudes $\tilde{b}_k$ in the wave-packet basis. The idea is to use short laser pulses to transfer a chosen amplitude to the ground state for time-resolved processing.

Consider a broadband laser pulse with a spectral width $\sim d/T_K$ that couples all the Rydberg levels in Eq. (16) to the ground state $|g\rangle$ in the atom. If the pulse is transform-limited, it has a temporal width less than T_K/d, and we can to good approximation ignore the free Kepler evolution of the wave-packet amplitudes shown in Eq. (23). Only the amplitude $\tilde{b}_0$ changes significantly during the pulse, corresponding to the wave-packet state $|0\rangle_\tau$ nearest the atomic core. This state undergoes Rabi oscillations with the ground state [11],

$$\dot{b}_g \cong \frac{i}{2} f(t)\tilde{\Omega}_0 \exp(-i\Delta_0 t)\tilde{b}_0, \tag{24}$$

$$\dot{\tilde{b}}_0 \cong \frac{i}{2} f(t)\tilde{\Omega}_0 \exp(i\Delta_0 t) b_g. \tag{25}$$

where $f(t)$ is the pulse profile, $\Delta_0 = \omega_0 - \omega$ is the detuning of the center frequency ω of the pulse from the average Rydberg frequency, and $\tilde{\Omega}_0$ is proportional to the average of the Rabi frequencies Ω_{gj} for the ground-to-Rydberg transitions,

$$\tilde{\Omega}_0 = \frac{1}{\sqrt{d}} \sum_j \Omega_{gj}. \tag{26}$$

A localized wave packet behaves classically for $t \sim T_K$, and the strong coupling to the laser field near the core can be understood as a large momentum transfer to the electron near the nucleus. The rate at which energy is absorbed from the field $\mathbf{E}$ is proportional to $\mathbf{p}\cdot\mathbf{E}$, and the electron momentum $\mathbf{p}$ is maximum at the inner turning point.

The two-level system of Eqs. (24) and (25) allows selective wave-packet processing in the atom. In particular, it allows phase control of individual wave-packet states in the Rydberg basis, as needed to implement $\mathcal{B}_{lm}$. To see this, note that a π-pulse of duration less than T_K/d de-excites only that part of the Rydberg wave function associated with a *single* wave-packet amplitude $\tilde{b}_k$, creating a 'dark' wave packet in its place in the Rydberg basis.

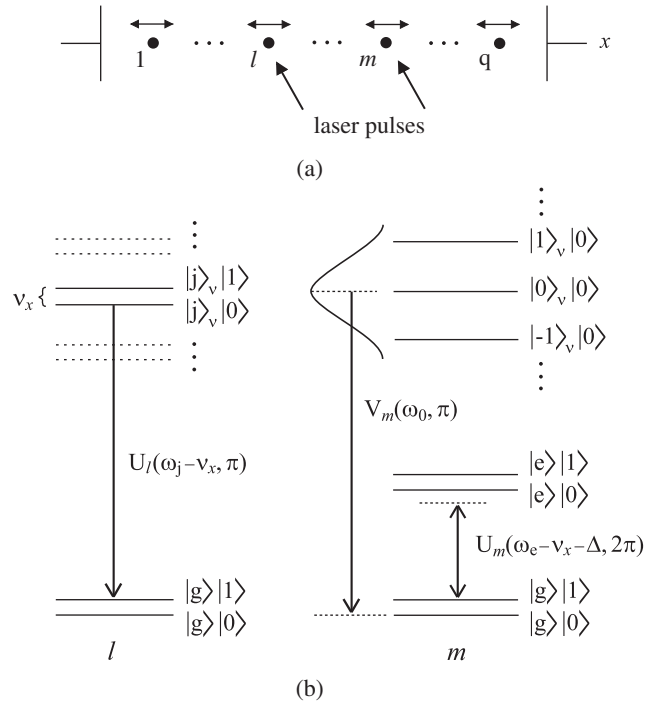

FIG. 3. Phase-gate implementation. (a) Ion trap with pulses applied to ions l (control) and m (target). (b) Level scheme in each ion, with Rydberg levels j and auxiliary levels g and e. Three types of pulses used: $U_l(\omega_j-\nu_x,\pi)$, $V_m(\omega_0,\pi)$, and $U_m(\omega_e-\nu_x-\Delta,2\pi)$. See text for details.

The phase of $\tilde{b}_k$ in the ground state can be controlled by a narrow-band 2π-pulse that couples this state to an auxiliary energy level in the atom (level e in figure 3). The phase-shifted amplitude can be restored to the Rydberg basis at a time commensurate with when the dark wave-packet state returns to the atomic core. This accomplishes a phase shift of a selected wave-packet state in the target atom.

Since the wave-packet basis is not stationary, the time between successive interactions with the Rydberg basis is dictated by the free atomic time scales. This time interval has to an integer number of Kepler periods during which the Rydberg state has not incurred much dispersion, or alternately, when the free time evolution undergoes a revival in the Schrödinger picture. This ensures that the decomposition of the Rydberg wave function in the wave-packet basis has not changed appreciably between pulses.

4. PHASE GATE IN THE LINEAR ION TRAP

Consider an implementation of the two-qudit phase gate $\mathcal{B}_{lm}$ in the linear ion-trap scheme for quantum computing [12]. Assuming that d energy levels in each trapped ion represent a qudit, consider a series of laser pulses applied to ions l and m in the trap, as illustrated in figure 3(a). Our goal is to control the phases of the

wave-packet states $|k\rangle_\tau$ in the mth ion conditional on the energy eigenstates $|j\rangle_\nu$ in the lth ion, as required by Eq. (21).

The ions are assumed to be in the vibrational ground state and oscillate synchronously in the center-of-mass normal mode in the trap. Assuming that the interaction field has a standing-wave pattern along the trap axis, two kinds of interactions have been proposed in this scheme, labeled U and V [12]. The V interaction arises when the ion is at the antinode of the standing wave, and the laser resonantly couples two internal states in the ion according to the unitary evolution operator

$$\hat{V}(t) = \exp\left[it\frac{\Omega}{2}(\hat{\sigma}^\dagger + \hat{\sigma})\right], \tag{27}$$

where Ω is the Rabi frequency and $\hat{\sigma}$ is the lowering operator for the atomic transition. Alternately, the U interaction arises when the ion is at the node of the standing wave and the laser is detuned off resonance to an atomic transition by the trap frequency ν_x. We consider the lowest two trap states, $|0\rangle$ and $|1\rangle$. For atomic levels g and e, where e is the upper level, we find that the states $|g\rangle|1\rangle$ and $|e\rangle|0\rangle$ are coupled by the unitary operator

$$\hat{U}(t) = \exp\left[-it\frac{\eta}{\sqrt{q}}\frac{\Omega}{2}(\hat{\sigma}^\dagger\hat{a} + \hat{\sigma}\hat{a}^\dagger)\right], \tag{28}$$

where $\hat{a}$ is the trap lowering operator and q is the number of ions in the trap. The Lamb-Dicke parameter η is defined as

$$\eta = k_x\sqrt{\frac{\hbar}{2m\nu_x}}, \tag{29}$$

where m is the mass of each ion, and k_x is the wave vector along the trap axis. The unitary evolution in Eq. (28) is valid in the limit that $\eta \ll 1$.

Consider the two-ion Rydberg wave function at some time t_0 when the trap has been initialized to $|0\rangle$,

$$|\Psi(t_0)\rangle = \sum_{j'}\sum_{k'} c_{j'k'}(t_0)\,|j',k'\rangle|0\rangle, \tag{30}$$

where we use the abbreviation $|j'\rangle_\nu|k'\rangle_\tau = |j',k'\rangle$, and the summations over j' and k' run over the d components of the energy-level and wave-packet bases in ions l and m respectively. The coefficients $c_{j'k'}$ are the Schrödinger picture amplitudes whose free time evolution has two contributions, one due to the phase evolution of the energy levels in the lth ion, and another due to the periodic evolution of the wave-packet amplitudes in the mth ion. We have to keep these contributions in mind as we pursue a phase gate in the hybrid basis.

When the kth wave-packet element in the mth ion is near the atomic core, the methods described in section 3 3.2 can be used to transfer the corresponding amplitudes $c_{j'k}$ to the ground state $|g\rangle$ in the ion. This is done by applying a broadband π-pulse of the V type, denoted by $V_m(\omega_0,\pi)$ in figure 3(b). The pulse spectrum is centered on the mean frequency ω_0 and has a duration less than T_K/d that is an integer multiple of $\pi/\tilde{\Omega}_0$. This only affects the wave-packet state nearest the atomic core, denoted by $k' = k$, and leaves the two ions in the state

$$\begin{aligned}|\Psi(t_1)\rangle &\\ &= \sum_{j'}\left[c_{j'k}(t_1)\,|j',g\rangle|0\rangle + \sum_{k'\neq k} c_{j'k'}(t_1)\,|j',k'\rangle|0\rangle\right]\\ &= |\Psi_k(t_1)\rangle + \sum_{j'}\sum_{k'\neq k} c_{j'k'}(t_1)\,|j',k'\rangle|0\rangle.\end{aligned} \tag{31}$$

The second term in Eq. (31) represents that part of the wave function in the mth ion that is left in the Rydberg manifold, and we suppress this term briefly. The first term corresponds to the kth wave-packet state that has been de-excited, which can be written as

$$\begin{aligned}|\Psi_k(t_1)\rangle &= \sum_{j'} c_{j'k}(t_1)\,|j',g\rangle|0\rangle\\ &= c_{jk}(t_1)\,|j,g\rangle|0\rangle + \sum_{j'\neq j} c_{j'k}(t_1)\,|j',g\rangle|0\rangle,\end{aligned} \tag{32}$$

where a particular energy level j is taken out of the j' summation. We seek to de-excite this level to the ground state in the lth ion, conditional on exciting the trap. This is done by applying a narrow-band π-pulse of the U type to the lth ion, which has a pulse duration that is an integer multiple of $\pi/(\eta\Omega_{gj}/\sqrt{q})$. The laser frequency is tuned to ω_j for the jth Rydberg level. This pulse is labeled $U_l(\omega_j - \nu_x, \pi)$ in figure 3(b), and transforms $|\Psi_k(t_1)\rangle$ to

$$|\Psi_k(t_2)\rangle = c_{jk}(t_2)\,|g,g\rangle|1\rangle + \sum_{j'\neq j} c_{j'k}(t_2)\,|j',g\rangle|0\rangle, \tag{33}$$

where the coefficients have evolved in phase from t_1 to t_2 due to the free time evolution of the energy levels in the Schrödinger picture. Equation (33) shows that the trap is excited only when both ions are in the ground state $|g,g\rangle$, corresponding to the initial state $|j,k\rangle$ at time t_0. Hence, the U pulse has created entanglement between the trap state and the internal states of the two ions.

To implement $\mathcal{B}_{lm}$, we need to shift the phase of $|j,k\rangle$ by ϕ_{jk} according to Eq. (21). In state $|\Psi_k(t_2)\rangle$, this corresponds to evolving the phase of $|g,g\rangle|1\rangle$ by ϕ_{jk} without affecting the other basis states. To do this, consider the auxiliary level e in the mth ion shown in figure 3(b). Applying a U pulse of 2π duration couples states $|g\rangle|1\rangle$ and $|e\rangle|0\rangle$ in the mth ion. For a laser detuning of Δ, the interaction phase of $|g,g\rangle|1\rangle$ evolves by an integer multiple of $\pi(1+\Delta/\Omega_{ge})$, which can be controlled to achieve ϕ_{jk}. This pulse is denoted $U_m(\omega_e - \nu_x - \Delta, 2\pi)$ in the figure, and transforms $|\Psi_k(t_2)\rangle$ to

$$\begin{aligned}|\Psi_k(t_3)\rangle &= c_{jk}(t_3)\exp(i\phi_{jk})\,|g,g\rangle|1\rangle\\ &\quad + \sum_{j'\neq j} c_{j'k}(t_3)\,|j',g\rangle|0\rangle,\end{aligned} \tag{34}$$

giving a controlled phase shift ϕ_{jk} to the state $|g,g\rangle|1\rangle$ as desired. We now reverse the operation that took us from $|\Psi_k(t_1)\rangle$ to $|\Psi_k(t_2)\rangle$ by applying $U_l(\omega_j-\nu_x,\pi)$ again to the lth ion, creating

$$|\Psi_k(t_4)\rangle = c_{jk}(t_4)\exp(i\phi_{jk})\,|j,g\rangle|0\rangle + \sum_{j'\neq j} c_{j'k}(t_4)\,|j',g\rangle|0\rangle. \tag{35}$$

Lastly, the mth ion state $|g\rangle$ is restored to $|k\rangle_\tau$ by applying $V_m(\omega_0,\pi)$ again at a time that is commensurate with when the 'dark' radial wave-packet element corresponding to k returns to the atomic core. Since this is a V pulse, it does not affect the trap. The resulting state is

$$|\Psi_k(t_5)\rangle = c_{jk}(t_5)\exp(i\phi_{jk})\,|j,k\rangle|0\rangle + \sum_{j'\neq j} c_{j'k}(t_5)\,|j',k\rangle|0\rangle. \tag{36}$$

The $k'\neq k$ terms in Eq. (31) are unaffected by the combination of the five pulses used above. Including their contribution to the final wave function, we get

$$|\Psi(t_5)\rangle = c_{jk}(t_5)\exp(i\phi_{jk})\,|j,k\rangle|0\rangle + \sum_{j'\neq j}\sum_{k'\neq k} c_{j'k'}(t_5)\,|j',k'\rangle|0\rangle. \tag{37}$$

Comparing Eqs. (30) and (37), we see that the sequence of five pulses,

$$V_m(\omega_0,\pi)\,U_l(\omega_j-\nu_x,\pi)\,U_m(\omega_e-\nu_x-\Delta,2\pi)\,U_l(\omega_j-\nu_x,\pi)\,V_m(\omega_0,\pi), \tag{38}$$

accomplishes a controlled phase shift of the hybrid state $|j,k\rangle = |j\rangle_\nu|k\rangle_\tau$, as desired. This procedure is repeated for each of the d^2 states in the two ions, leading to the phase gate $\mathcal{B}_{lm}$ in mixed energy-level and wave-packet bases.

The coefficients $c_{j'k'}(t_5)$ are different from $c_{j'k'}(t_0)$ due to the phase evolution of the energy levels in both ions during the time interval t_5-t_0. This is also responsible for the non-stationarity of the wave-packet basis, which makes this procedure sensitive to when the kth wave-packet amplitude in the mth ion is de-excited from, and excited to, the Rydberg manifold. The time interval between the two V_m pulses in the sequence is determined by the free atomic time scales governing the classical or revival dynamics of the wave packets. By appropriate timing of these pulses, we can implement a conditional phase-shift between the two atoms.

5. CONCLUSION

This paper shows that the quantum FFT can be simplified using a multilevel wave-packet approach to its implementation. In atomic systems, the basic logic gate is a multilevel Fourier transform $\mathcal{A}_m$ in each atom, which is equivalent to a change of basis from energy levels to wave packets. Such an implementation takes advantage of the natural Fourier transform relation between energy and time in quantum mechanics. The FFT then reduces to a series of two-qudit phase gates $\mathcal{B}_{lm}$ in hybrid bases, which we have considered in the context of the linear ion-trap scheme for quantum computing.

The advantage of the multilevel approach is a reduction in the number of entangled quantum systems (e.g. trapped ions) by a factor of $\log_2 d$ compared to the binary case. For the same reason, the number of logic gates needed to simulate DFT_N is fewer by a factor of $(\log_2 d)^2$, as seen by comparing Eqs. (4) and (9). However, this comes at the cost of larger elementary gates, up to d^2-dimensional in the case of $\mathcal{B}_{lm}$. The trade-off in computation time depends very much on the particular implementation scheme used, which dictates the physical time taken to perform each gate.

The bottleneck for the gate operation time in the linear ion-trap scheme is the trap frequency ν_x [17], typically kHz to MHz, which limits the speed of the narrow-band U pulses. This is due to the need for selective entanglement between the internal state of the ion and its motional state in the trap. By comparison, the Rydberg atomic time scales are much faster, typically in the ns to μs range, allowing much faster execution times in principle for the phase-gate protocol given in section 4.

There are two advantages to a wave-packet approach to multilevel processing. One is the quantum Fourier transform itself, which is integral to the approach and key to quantum computing. The other is the feasibility of the control scheme for atomic systems. Universal control of multiple energy levels in the atom requires multiple lasers tuned to the neighbouring transitions [9]. This is much easier in the time domain, where wave-packet transforms can be achieved by controlling the timing and durations of a sequence of laser pulses. The implementation of the quantum FFT in multilevel systems is thus made more feasible using wave-packet methods.

This work was supported by the Army Research Office through the MURI Center for Quantum Information.

* Electronic Address: amuthuk@optics.rochester.edu

[1] R. Jozsa, Proc. Roy. Soc. Lond. A **454**, 323 (1998).
[2] P. W. Shor, SIAM J. Comp. **26**, 1484 (1997).
[3] R. L. Rivest, A. Shamir and L. Adleman, Commun. of A.C.M. **21**, 120 (1978).
[4] D. Coppersmith, IBM Res. Report RC 19642, T.J. Watson Research Center, Yorktown Heights, NY, 1994.
[5] J. W. Cooley and J. W. Tukey, Math. Computation **19**, 297 (1965).
[6] R. B. Griffiths and C. Niu, Phys. Rev. Lett. **76**, 3228 (1996).
[7] R. Cleve and J. Watrous, in *Proc. 41st Annual Symp.*

Found. Comp. Sci. (IEEE, Los Alamitos, CA, 2000), p. 526. Also at quant-ph/0006004.
[8] A. Barenco et al., Phys. Rev. A **54**, 139 (1996).
[9] A. Muthukrishnan and C. R. Stroud, Jr., Phys. Rev. A **62**, 52309 (2000).
[10] Bowden, C. M., Chen, G., Diao, Z., and Klappenecker, A., quant-ph/0007122 at xxx.lanl.gov.
[11] Muthukrishnan, A., and Stroud, Jr., C. R., quant-ph/0106165 at xxx.lanl.gov.
[12] J. I. Cirac and P. Zoller, Phys. Rev. Lett. **74**, 4091 (1995).
[13] A. Ekert and R. Josza, Rev. Mod. Phys. **68**, 733 (1996).
[14] R. Jozsa, to appear in *Geometric Issues in the Foundations of Science*, eds. S. Huggett et al. (Oxford Univ. Press). Also at quant-ph/9707034.
[15] J. Parker and C. R. Stroud, Jr., Phys. Rev. Lett. **56**, 716 (1986).
[16] A. ten Wolde et al., Phys. Rev. Lett. **61**, 2099 (1988).
[17] D. Jonathan, M. B. Plenio and P. L. Knight, Phys. Rev. A **62**, 42307 (2000).